

Observation of suppressed terahertz absorption in photoexcited graphene

A. J. Frenzel,^{1,2} C. H. Lui,¹ W. Fang,³ N. L. Nair,¹ P. K. Herring,^{1,2} P. Jarillo-Herrero,¹ J. Kong,³ and N. Gedik^{1, a)}

¹⁾Department of Physics, Massachusetts Institute of Technology, Cambridge, Massachusetts 02139.

²⁾Department of Physics, Harvard University, Cambridge, Massachusetts 02138.

³⁾Department of Electrical Engineering and Computer Science, Massachusetts Institute of Technology, Cambridge, Massachusetts 02139.

(Dated: 7 May 2019)

When light is absorbed by a semiconductor, photoexcited charge carriers enhance the absorption of far-infrared radiation due to intraband scattering. We observe the opposite behavior in monolayer graphene, a zero-gap semiconductor with linear dispersion. By using time domain terahertz (THz) spectroscopy in conjunction with optical pump excitation, we observe a reduced absorption of THz radiation in photoexcited graphene. The measured spectral shape of the differential optical conductivity exhibits strongly non-Drude behavior. We discuss the influence of hot optical phonons, thermally broadened carrier distribution, and stimulated emission of THz radiation on the low-frequency non-equilibrium optical response of graphene.

Two-dimensional graphene is characterized by its distinctive Dirac electronic structure and the associated remarkable optical properties, specifically, a strong and broadband optical absorption from far-infrared to ultraviolet wavelengths.^{1–3} The unique gapless band structure of graphene, together with the great tunability of its Fermi level by electrical gating, has made it a promising material for novel optoelectronic applications in the far-infrared regime. For instance, recent research has demonstrated graphene to be an efficient terahertz (THz) modulator^{4–6} and a possible gain medium for a THz laser.⁷ Optical pump excitation has been shown to effectively modulate the THz response of graphene. In particular, recent studies report enhanced absorption of THz radiation in optically pumped graphene.^{8–11} In these works, the observation was understood by considering Drude absorption with a fixed scattering rate, which typically increases with the population of photoexcited carriers. However, the small Fermi energy and linear dispersion of graphene suggest that non-Drude behavior is likely to occur, and hot optical phonons may alter carrier scattering rates. These effects on the low-frequency optical response of graphene under non-equilibrium conditions have yet to be investigated.

In this paper, we present optical-pump THz-probe^{12,13} measurements of the ultrafast far-infrared response of large-area monolayer graphene grown by chemical vapor deposition (CVD). We observe a transient decrease of THz absorption in graphene subject to pulsed optical excitation, a result in contrast with the increased absorption reported previously in epitaxial graphene and totally unexpected from a standard Drude model.^{9–11} In addition, the differential THz conductivity spectrum deviates significantly from the Drude form. We propose that the observed anomalous THz bleaching may arise from additional scattering between charge carriers and hot optical phonons, thermal broadening of the electron distribution,

or possible stimulated emission of THz radiation near the Dirac points.

The apparatus and procedure used in our optical-pump THz-probe experiment are similar to that described in Ref (12). The laser source is an amplified mode-locked Ti:Sapphire system that provides pulses of central wavelength 800 nm, pulse duration \sim 100 fs and repetition rate 5 kHz. The THz probe pulses were generated by optical rectification of the 800 nm pulses in a 1 mm-thick ZnTe crystal and detected by electro-optic sampling of the 800 nm pulses in a 0.1 mm-thick ZnTe crystal. The spot sizes of the 800 nm pump beam and the THz probe beam on the sample were \sim 5 mm and \sim 2 mm, respectively, to ensure approximately homogeneous pumping of the probed sample area. Measurements presented here were performed in the low-fluence regime (incident pump fluence \sim 10 μ J/cm^{−2}) at room temperature and in high vacuum (pressure $<$ 10^{−5} Torr). Using the two-temperature model of Ref (14), we estimate that under our experimental conditions, the maximum transient electronic temperature is \lesssim 1000 K and the full equilibrium heating of the lattice is negligible.

Monolayer graphene samples were grown by CVD¹⁵ on copper foils and subsequently transferred to different substrates, including sapphire, *z*-cut crystalline quartz and borosilicate glass. The monolayer thickness and the sample quality of the CVD graphene were characterized by Raman spectroscopy¹⁶ (inset of Fig. 1). We have measured the THz absorption spectrum of the CVD samples without optical excitation and extracted the complex optical conductivity of graphene using the method described in Ref (17). Fig. 1 displays the conductivity spectrum of a graphene sample on a quartz substrate at room temperature. The data can be fit well by the Drude formula with a Fermi energy $E_F \sim$ 300 meV and scattering rate $\Gamma \sim$ 3 THz (100 cm^{−1}), corresponding to a carrier density $n \sim 6 \times 10^{12}$ cm^{−2} and mobility $\mu = 2000$ cm²/V·s. These parameters are reasonable for doped CVD graphene on a substrate.^{4,5,18,19}

When we pump the graphene/quartz sample with 800 nm pulses, we observe a significant change in the trans-

^{a)}Electronic mail: gedik@mit.edu

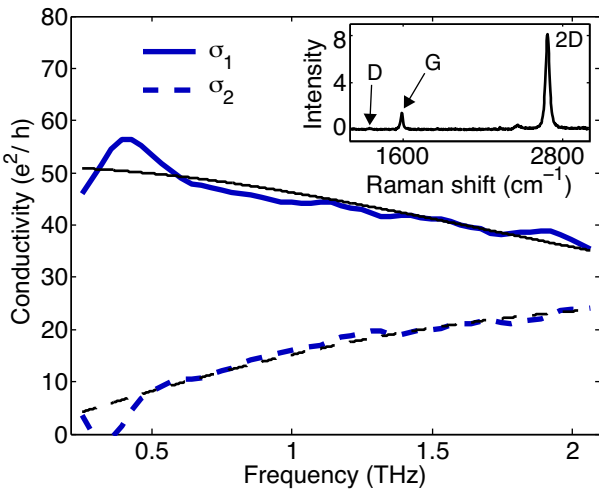


FIG. 1. (color) Complex optical conductivity of graphene from 0.21 to 2.1 THz. The measurement was performed at room temperature on monolayer CVD graphene on a quartz substrate without optical excitation. The blue solid and dashed lines are the real (σ_1) and imaginary (σ_2) part of the conductivity, respectively. The data can be described by the Drude model (thin black lines) with carrier scattering rate $\Gamma = 3$ THz. The inset shows a typical Raman spectrum of our CVD graphene (excitation wavelength 532 nm). The narrow Lorentzian line shape of the 2D mode confirms the monolayer thickness of the samples. The small D-mode signal indicates the high crystalline quality of the samples.

mitted THz probe pulses (Fig. 2a). Strikingly, the THz transmission is found to increase following pulsed excitation. For a thin film deposited on a transparent substrate, the differential transmitted field ΔE , normalized to the equilibrium transmitted field E , is related to the differential optical conductivity $\Delta\sigma$ as¹⁷

$$\frac{\Delta E}{E} = - \left(\frac{Z_0}{n_s + 1} \right) \Delta\sigma \quad (1)$$

where n_s is the substrate refractive index and Z_0 the impedance of free space. Our observation of positive ΔE therefore corresponds to negative differential conductivity, or reduced absorption, in graphene. Fig. 2b displays the temporal dynamics of the pump-induced modulation of THz transmission, which are well described by an exponential decay with time constant $\tau = 1.7$ ps (Fig. 2b inset). It is firmly established that photoexcited charge carriers in graphene thermalize rapidly and relax most of their energy to a set of strongly coupled optical phonons within a few hundred femtoseconds.^{8,14,20-23} The equilibrated subsystem of electrons and optical phonons subsequently cools within a few picoseconds through the anharmonic decay of the optical phonons. We therefore attribute the observed dynamics of the THz response to the cooling of the coupled electron-phonon system.

We have also used Eq. (1) to extract the complex differential conductivity spectra ($\Delta\sigma = \Delta\sigma_1 + i\Delta\sigma_2$) from

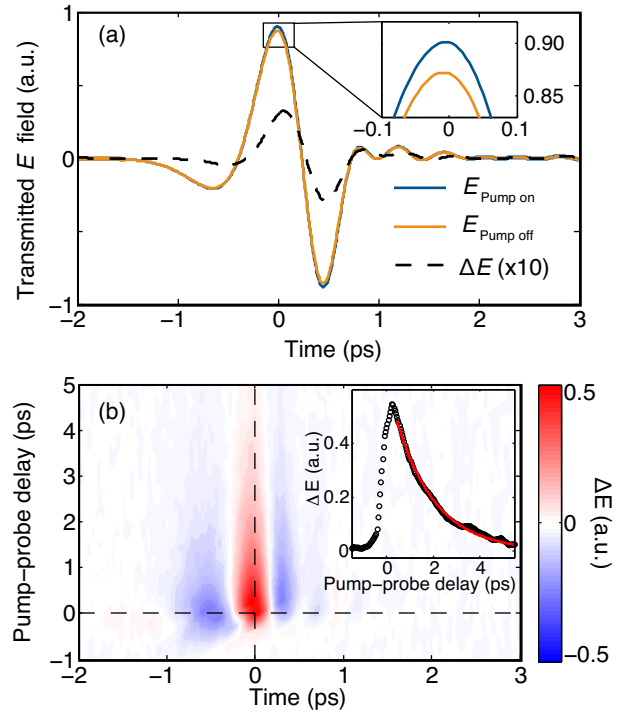


FIG. 2. (color) (a) Transmission of the THz electric field with (blue) and without (orange) simultaneous pump excitation. The dashed line, scaled by a factor of 10 for clarity, is the pump induced modulation of the transmitted electric field ΔE . The inset shows a zoomed-in view of the peak, indicating that ΔE corresponds to a pump-induced bleaching of the graphene sample. (b) Temporal dynamics of ΔE following optical pump excitation. The horizontal and vertical dashed lines are, respectively, the zero pump-probe delay time and the peak position of ΔE . Inset shows the temporal dynamics of the peak of ΔE (vertical dashed line in main panel). The red line is a single-exponential fit with time constant $\tau = 1.7$ ps. The peak value of the signal corresponds to $\Delta E/E \sim 5\%$.

the transmission data in Fig. 2b at different pump-probe delay times (Fig. 3a). We find that $\Delta\sigma_1$ remains negative for the whole decay process after pulsed excitation (Fig. 3a), and for the entire measured spectral range (see, for example, the spectrum at pump-probe delay 1 ps in Fig. 3b). We note that we have observed similar negative $\Delta\sigma$ for CVD graphene samples on different (sapphire, quartz and borosilicate glass) substrates, at temperatures ranging from 4 to 300 K, and in both ambient and vacuum conditions. We therefore believe it is an intrinsic property of doped graphene. The results are surprising because the intraband absorption of graphene is typically described by the Drude model with a constant scattering rate. Increasing the free carrier population by photoexcitation should lead to enhanced THz absorption, as observed in epitaxial graphene layers on SiC substrate,⁹⁻¹¹ as well as in traditional semiconductors such as GaAs¹² and Si.²⁴

Multiple processes may contribute to the sign and spectral shape of the measured differential THz conductivity

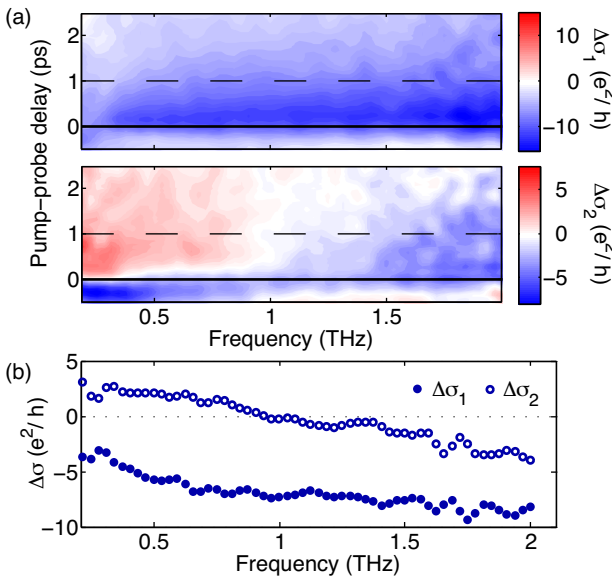


FIG. 3. (color) (a) Temporal dynamics of the real (upper panel) and imaginary (lower panel) parts of the differential THz conductivity of optically pumped monolayer graphene. The black lines denote zero pump-probe delay time. (b) Differential conductivity 1 ps after optical excitation (horizontal dashed lines in (a)). The filled and open dots circles the experimental real and imaginary parts of the conductivity, respectively.

in graphene (Fig. 3b). One possible mechanism, which can account for the sign but does not explain the shape, is an increase of the intraband scattering rate by optical pumping. In particular, because the photon energy of our pump laser (1.55 eV) is considerably larger than the optical phonon energy in graphene (~ 0.2 eV),²⁵ the relaxation of photoexcited charge carriers can efficiently produce a significant population of strongly coupled optical phonons.^{21–23} Additional electron-optical phonon scattering then suppresses intraband optical absorption, as has been observed in graphite.⁸ This mechanism is also responsible for current saturation in high-field transport in graphene devices.^{26–29} A recent THz-pump THz-probe study also shows signatures of increased intraband scattering due to heating the electron system with an intense THz pulse.³⁰ Another effect, which may contribute to the observed non-Drude spectral shape, is the broadened carrier distribution that results from the high transient temperature of the electronic system. While the Drude model assumes a constant (energy independent) scattering rate, the intraband optical absorption of a hot ($k_B T \sim \mu$) electron gas with linear dispersion cannot be accurately described by a single energy-independent scattering rate,³¹ but different scattering rates for electrons with different energies must be considered. Alternatively, recent research has provided evidence that there is a transient regime of population inversion in graphene during the first few picoseconds after optical pump excitation,³² which could amplify a THz probe pulse.³³ Such stimu-

lated emission of THz radiation may also contribute to the observed negative differential conductivity.

In summary, we have observed reduced absorption of THz radiation and a non-Drude differential conductivity spectrum in graphene subject to pulsed optical excitation. Our results may be explained by additional scattering due to hot phonons, a thermally broadened carrier distribution, or possible stimulated emission in graphene following optical pumping. Further studies at higher fluence and in samples with different Fermi energies may help to clarify the roles played by each of these mechanisms.

Upon completion of this work, we became aware of a similar work by another group.³⁴ We did not, however, observe any influence of the ambient environment on the sign of the differential conductivity, as reported therein.

The authors acknowledge helpful discussions with N.M. Gabor, J.C.W. Song, and H.Y. Hwang. This research is supported by Department of Energy Office of Basic Energy Sciences Grant No DE-SC0006423. A.J.F. acknowledges support from NSF GRFP. P.J.H. acknowledges support by the Air Force Office of Scientific Research and the Office of Naval Research GATE MURI. This work made use of MIT's MRSEC Shared Experimental Facilities supported by the National Science Foundation under award No. DMR-0819762 and of Harvard's Center for Nanoscale Systems (CNS), supported by the National Science Foundation under grant No. ECS-0335765.

- ¹A. K. Geim and K. S. Novoselov, *Nature Materials* **6**, 183 (2007).
- ²F. Bonaccorso, Z. Sun, T. Hasan, and A. C. Ferrari, *Nature Photonics* **4**, 611 (2010).
- ³K. F. Mak, L. Ju, F. Wang, and T. F. Heinz, *Solid State Comm.* **152**, 1341 (2012).
- ⁴J. Horng, C.-F. Chen, B. Geng, C. Girit, Y. Zhang, Z. Hao, H. Bechtel, M. Martin, A. Zettl, M. Crommie, Y. Shen, and F. Wang, *Phys. Rev. B* **83**, 1 (2011).
- ⁵L. Ren, Q. Zhang, J. Yao, Z. Sun, R. Kaneko, Z. Yan, S. Nanot, Z. Jin, I. Kawayama, M. Tonouchi, J. M. Tour, and J. Kono, *Nano Lett.* **12**, 3711 (2012).
- ⁶I. Maeng, S. Lim, S. J. Chae, Y. H. Lee, H. Choi, and J.-H. Son, *Nano Lett.* **12**, 551 (2012).
- ⁷T. Otsuji, S. A. Boubanga Tombet, A. Satou, H. Fukidome, M. Suemitsu, E. Sano, V. Popov, M. Ryzhii, and V. Ryzhii, *MRS Bulletin* **37**, 1235 (2012).
- ⁸T. Kampfrath, L. Perfetti, F. Schapper, C. Frischkorn, and M. Wolf, *Phys. Rev. Lett.* **95**, 187403 (2005).
- ⁹P. A. George, J. Strait, J. Dawlaty, S. Shivaraman, M. Chandrashekhar, F. Rana, and M. G. Spencer, *Nano Lett.* **8**, 4248 (2008).
- ¹⁰H. Choi, F. Borondics, D. A. Siegel, S. Y. Zhou, M. C. Martin, A. Lanzara, and R. A. Kaindl, *Appl. Phys. Lett.* **94**, 172102 (2009).
- ¹¹J. H. Strait, H. Wang, S. Shivaraman, V. Shields, M. Spencer, and F. Rana, *Nano Lett.* **11**, 4902 (2011).
- ¹²M. C. Beard, G. M. Turner, and C. A. Schmuttenmaer, *J. Appl. Phys.* **90**, 5915 (2001).
- ¹³R. Ulbricht, E. Hendry, J. Shan, T. Heinz, and M. Bonn, *Rev. Mod. Phys.* **83**, 543 (2011).
- ¹⁴C. H. Lui, K. F. Mak, J. Shan, and T. Heinz, *Phys. Rev. Lett.* **105**, 127404 (2010).
- ¹⁵X. Li, W. Cai, J. An, S. Kim, J. Nah, D. Yang, R. Piner, A. Velamakanni, I. Jung, E. Tutuc, S. K. Banerjee, L. Colombo, and R. S. Ruoff, *Science* **324**, 1312 (2009).

¹⁶A. C. Ferrari, J. C. Meyer, V. Scardaci, C. Casiraghi, M. Lazzari, F. Mauri, S. Piscanec, D. Jiang, K. S. Novoselov, S. Roth, and A. K. Geim, Phys. Rev. Lett. **97**, 1 (2006).

¹⁷M. C. Nuss and J. Orenstein, in *Millimeter and Submillimeter Wave Spectroscopy of Solids*, edited by G. Grüner (Springer, Berlin, 1998) Chap. 2, pp. 7–50.

¹⁸H. Yan, F. Xia, W. Zhu, M. Freitag, C. Dimitrakopoulos, A. A. Bol, G. Tulevski, and P. Avouris, ACS Nano **5**, 9854 (2011).

¹⁹C. Lee, J. Y. Kim, S. Bae, K. S. Kim, B. H. Hong, and E. J. Choi, Appl. Phys. Lett. **98**, 071905 (2011).

²⁰S. Butscher, F. Milde, M. Hirtschulz, E. Malić, and A. Knorr, Appl. Phys. Lett. **91**, 203103 (2007).

²¹H. Yan, D. Song, K. F. Mak, I. Chatzakis, J. Maultzsch, and T. F. Heinz, Phys. Rev. B **80**, 121403(R) (2009).

²²K. Kang, D. Abdula, D. G. Cahill, and M. Shim, Phys. Rev. B **81**, 165405 (2010).

²³S. Wu, W.-T. Liu, X. Liang, P. J. Schuck, F. Wang, Y. R. Shen, and M. Salmeron, Nano Lett. **12**, 5495 (2012).

²⁴T. Suzuki and R. Shimano, Phys. Rev. Lett. **103**, 057401 (2009).

²⁵S. Piscanec, M. Lazzari, F. Mauri, A. C. Ferrari, and J. Robertson, Phys. Rev. Lett. **93**, 185503 (2004).

²⁶A. Barreiro, M. Lazzari, J. Moser, F. Mauri, and A. Bachtold, Physical Review Letters **103**, 2 (2009).

²⁷D.-H. Chae, B. Krauss, K. von Klitzing, and J. H. Smet, Nano Letters **10**, 466 (2010).

²⁸S. Berciaud, M. Y. Han, K. F. Mak, L. E. Brus, P. Kim, and T. F. Heinz, Phys. Rev. Lett. **104**, 227401 (2010).

²⁹V. Perebeinos and P. Avouris, Physical Review B **81**, 1 (2010).

³⁰H. Y. Hwang, N. C. Brandt, H. Farhat, A. L. Hsu, J. Kong, and K. A. Nelson, (2011), arXiv:1101.4985v1.

³¹N. W. Ashcroft and N. D. Mermin, *Solid State Physics* (Brooks Cole, 1976).

³²T. Li, L. Luo, M. Hupalo, J. Zhang, M. C. Tringides, J. Schmalian, and J. Wang, Physical Review Letters **108**, 167401 (2012).

³³V. Ryzhii, M. Ryzhii, and T. Otsuji, J. Appl. Phys. **101**, 083114 (2007).

³⁴C. J. Docherty, C.-T. Lin, H. J. Joyce, R. J. Nicholas, L. M. Herz, L.-J. Li, and M. B. Johnston, Nature Comm. **3**, 1228 (2012).